

Manfred Cejna, MD
Johannes M. Breuss, PhD
Helga Bergmeister, DVM, MD
Rainer de Martin, PhD
Zhongying Xu, MD
Mario Grgurin, MD
Udo Losert, DVM
Hanns Plenck, Jr, MD
Bernd R. Binder, MD
Johannes Lammer, MD

Index terms:

Animals
Arteriosclerosis, 9*.721²
Experimental study
Genes and genetics
Stents and prostheses, 981.1282,
981.1286

Published online before print
10.1148/radiol.2233011002
Radiology 2002; 223:702–708

Abbreviations:

ANOVA = analysis of variance
CMV = cytomegalovirus
GFP = green fluorescent protein
PBS = phosphate-buffered saline

¹ From the Departments of Radiology, Division of Angiography and Interventional Radiology (M.C., Z.X., M.G., J.L.) and Vascular Biology and Thrombosis Research (J.M.B., R.d.M., B.R.B.), the Center of Biomedical Research (H.B., U.L.), and Bone and Biomaterials Research, Institute for Histology and Embryology (H.P.), Vienna Medical School, Währinger Gürtel 18-20, A-1090 Vienna, Austria. Received June 6, 2001; revision requested July 20; final revision received November 9; accepted December 11. Supported in part by a Cardiovascular and Interventional Radiological Society of Europe research grant (1999), Mallinckrodt and Schering, and Boston Scientific. **Address correspondence to M.C.** (e-mail: manfred.cejna@univie.ac.at).

² 9*. Vascular system, location unspecified

© RSNA, 2002

Author contributions:

Guarantors of integrity of entire study, M.C., J.M.B., H.B.; study concepts, M.C., J.L., B.R.B., U.L., R.d.M.; study design, M.C., J.L., B.R.B., J.M.B., H.P., R.d.M., U.L.; literature research, M.C., M.G., Z.X.; clinical studies, M.C., J.M.B., H.B., M.G., Z.X.; experimental studies, M.C., M.G., J.M.B., Z.X., H.B.; data acquisition and analysis/interpretation, M.C., J.M.B., H.B., M.G., Z.X.; statistical analysis, M.C., J.M.B., H.B.; manuscript preparation, definition of intellectual content, editing, revision/review, and final version approval, all authors.

Inhibition of Neointimal Formation after Stent Placement with Adenovirus-mediated Gene Transfer of I κ B α in the Hypercholesterolemic Rabbit Model: Initial Results¹

PURPOSE: To evaluate the feasibility and efficacy of the local application of a replication-defective adenovirus construct for the expression of the antiinflammatory protein I κ B α , inhibitor of nuclear factor κ B (NF- κ B), to reduce neointimal formation after stent placement.

MATERIALS AND METHODS: Nitinol stents were implanted in the iliac arteries of hypercholesterolemic rabbits, followed by balloon dilation (30 seconds at 6 atm). Local adenovirus-mediated transfer of I κ B α (3 mL of 10⁹ plaque-forming units per milliliter at 6 atm) was performed and compared with three control groups: stent alone, stent plus local delivery of phosphate-buffered saline (PBS) (3 mL at 6 atm), and stent plus local delivery of control adenovirus coding for green fluorescent protein (GFP) (3 mL of 10⁹ plaque-forming units per milliliter at 6 atm). A multichannel balloon was used for local drug delivery and balloon dilation. Animals were sacrificed 1 or 4 weeks after treatment. Effective transfection was demonstrated with immunofluorescence staining. Angiographic patency and luminal diameter were evaluated at quantitative angiography. Luminal and neointimal areas were measured on surface-stained ground sections with methylmethacrylate embedding and the cutting-grinding technique.

RESULTS: All vessels with stents were patent at angiography. Neointimal area was negligible in all groups 1 week after stent placement (range, 0.42–0.52 mm²; $P = .44$; analysis of variance). Neointimal formation was demonstrated in all groups 4 weeks after implantation but was significantly reduced with I κ B α treatment compared with treatment with stent alone (by 22%, from 2.80 mm² \pm 0.20 to 2.28 mm² \pm 0.14, $P = .05$), stent plus PBS (by 43%, from 3.26 mm² \pm 0.25 to 2.28 mm² \pm 0.14, $P = .005$), and stent plus GFP (by 53%, from 2.32 mm² \pm 0.19 to 1.51 mm² \pm 0.08, $P < .005$).

CONCLUSION: Local adenovirus-mediated I κ B α gene transfer has the potential to reduce intimal hyperplasia after stent placement.

Neointimal formation is a general response of the arterial wall to the injury of balloon dilation (1) and stent implantation (2). Although stents have been shown to mitigate the risk of restenosis in large clinical trials (3,4), thus preventing recoil and remodeling, in-stent restenosis is still a frequent and often intractable clinical problem (2–4).

Inflammatory cells play a key role in postinjury intimal hyperplasia. Soon after balloon angioplasty (5) or placement of stents (6), monocytes are recruited at the injury site, where they become activated macrophages. The extent of macrophage infiltration of lesions with stents has been correlated with subsequent intimal growth (7). Moreover, in patients with

coronary artery disease, the presence of activated circulating monocytes before angioplasty predicts more severe late luminal stenosis (8). Local gene transfer has been effective in animal models of neointimal formation (9–11). These data suggest that deactivation of the inflammatory cascade and inhibition of smooth muscle cell proliferation may limit postinjury intimal hyperplasia and in-stent restenosis.

Transcription factors, which are activated by means of mitogenic factors that lead to up regulation of cytokines and/or adhesion molecules, are key downstream regulators of the cellular reaction to trauma. The transcription factor, nuclear factor κ B (NF- κ B), is involved in mediating local procoagulant activity and local inflammation (12,13). Various stimuli (interleukin 1, tumor necrosis factor, and lipopolysaccharides) lead to phosphorylation and deactivation of the cytosolic inhibitor of NF- κ B, I κ B α , thereby freeing NF- κ B to translocate to the nucleus and activate transcription of inflammatory response genes (13). NF- κ B is also involved in the control of apoptosis and proliferation of smooth muscle cells (14,15). Adenovirus-mediated overexpression of I κ B α prevents nuclear translocation of NF- κ B, shuts down the antiapoptotic effect of NF- κ B, and prevents smooth muscle cell proliferation (14,15). The purpose of our study was to evaluate the feasibility and efficacy of the local application of a replication-defective adenovirus construct for I κ B α expression to reduce neointimal formation after stent placement.

MATERIALS AND METHODS

Recombinant Adenoviral Vectors

Replication-defective recombinant adenoviral vectors, rAdCMV.I κ B α or rAdCMV.GFP, based on human adenovirus 5 serotype containing the coding sequence for I κ B α or green fluorescent protein (GFP) under the cytomegalovirus (CMV) promoter were created and used as described previously (13,16). The first adenine-thymidine-guanosine codon of the I κ B α complementary DNA was replaced with a Bacillus amylolyticus type II restriction endonuclease (BamHI) restriction site by using polymerase chain reaction. A double-stranded oligonucleotide encoding an initiator methionine followed by the simian virus SV40 large T antigen nuclear localization signal and three glycine residues as a flexible spacer was ligated into the newly generated BamHI site. The construct was sequenced

to exclude possible errors generated during the amplification procedure, ligated into the vector pACCMVpLpASR+, and cotransfected with pJM17, a plasmid containing the adenoviral genome with a deletion in the E1 region, into 293 cells by using LipofectaminPlus (Gibco-BRL; Invitrogen, Carlsbad, Calif). Clones obtained after subcloning on 293 cells were tested for I κ B α expression with Western blotting by using an anti-MAD-3 antibody (Santa Cruz Biotechnology, Santa Cruz, Calif) at a dilution of 1:1,500. A large batch of the recombinant adenovirus was purified by means of two consecutive cesium chloride centrifugations.

Animal Preparation and Surgical Procedures

All animal care and handling were performed in accordance with the guidelines specified by the National Institutes of Health Guide for the Care and Use of Laboratory Animals and were approved by the local Institutional Animal Care and Use Committee of the University of Vienna. Only female New Zealand White rabbits older than 6 months, after completion of their growth period, and weighing between 3.5 and 4.0 kg were used. Hypercholesterolemia was induced with a diet of rabbit chow supplemented with 1.5% cholesterol and 7% peanut oil for 3 weeks prior to stent implantation. After stent implantation, the animals received a maintenance diet of standard rabbit chow mixed with supplemented chow (3:1). Cholesterol and triglyceride levels were measured at baseline, after completion of the induction, and at the end of the maintenance diet.

Anesthesia was induced with 30 mg per kilogram of body weight of ketamine (Ketanest; Parke-Davis, Vienna, Austria) and 2 mg/kg of xylazine (Xylazine-HCL; Boehringer Ingelheim, Vienna, Austria) administered intramuscularly. Before endotracheal intubation, anesthesia was deepened with intravenous application of ketamine and xylazine (100 mg of ketamine, 4 mg of xylazine, and 5 mL of sodium chloride) to effect, followed by intubation and volume-controlled ventilation with 1.5% isoflurane (Forane; Abbott, Vienna, Austria). After surgical preparation, a 6-F sheath (Radiofocus; Terumo Europe, Leuven, Belgium) was introduced into the carotid artery. Digital subtraction angiography was performed before and after the intervention.

At the end of the follow-up period, laparotomy was performed with general anesthesia. Rabbits were killed with an overdose of potassium and thiopental,

the distal aorta and the iliac vessels were removed en bloc.

Experimental Protocol

Prior to the start of the study, the safety and efficacy of local viral transfection with rAdCMV.GFP were evaluated in five animals at 1- and 4-week follow-up. We also evaluated effective local transfection with immunofluorescence and potential systemic transfection with samples of liver, kidney, and lung after sacrifice at the respective times. The actual experimental groups were stent only ($n = 4$, 1-week follow-up; $n = 4$, 4-week follow-up), stent plus phosphate-buffered saline (PBS) ($n = 3$, 1-week follow-up; $n = 4$, 4-week follow-up), stent plus I κ B α ($n = 3$, 1-week follow-up; $n = 4$, 4-week follow-up), and stent plus GFP ($n = 3$, 1-week follow-up only). A second series of experiments was performed to compare late effects (4 weeks after stent placement) of vessels treated with rAdCMV.GFP ($n = 3$) with those treated with rAdCMV.I κ B α ($n = 3$). To avoid potential cross flow and influences of systemic transfection in contralateral controls, adenoviral treatment was performed unilaterally without a contralateral negative control (Fig 1). Negative control stent implantation (stent alone or stent plus local delivery of PBS) was performed in ipsi- and contralateral iliac arteries in each control animal (Fig 1). In one animal, acute iliac artery occlusion immediately after stent placement and I κ B α treatment was demonstrated; the animal was excluded from the study.

Angiographic Procedure, Stent Implantation, and Quantitative Angiography

Digital subtraction angiography of the iliac arteries was performed with a mobile C-arm angiographic unit (Siremobil 2000; Siemens, Erlangen, Germany). Angiography was performed with a 4-F end-hole catheter (Cordis, Miami, Fla), which was placed in the distal abdominal aorta via a 0.018-inch guide wire (Boston Scientific, Natick, Mass). All angiographic examinations were performed with manual injection of 3 mL of iodinated contrast medium (300 mg of iodine per milliliter, ioversol [Optiray]; Mallinckrodt, Geffen, Germany) mixed with saline (2:1). The self-expanding nitinol stent (Symphony; Boston Scientific), which was 3.5 mm in diameter and 15 mm long (Fig 1), was implanted in the external iliac artery. A 6-F wide-lumen catheter (Envoy; Cordis) was positioned in

the distal external iliac artery, the guide wire was withdrawn. The self-expanding nitinol stent was manually inserted in the catheter, pushed distally with the 4-F end-hole catheter, then positioned and expanded with the withdrawal of the 6-F wide-lumen catheter. Then the 6-F wide-lumen and 4-F end-hole catheters were removed.

Local drug delivery was performed with the multichannel balloon positioned in the segment with the stent via a 0.014-inch guide wire (Boston Scientific). Balloon angioplasty (30 seconds at 5–6 atm) and local drug delivery (rAdCMV.GFP or rAdCMV. I κ B α [3 mL of 1×10^9 plaque-forming units per milliliter]) were performed with the multichannel balloon (3 \times 20 mm, Boston Scientific) (17) (Fig 1) and an inflator with a pressure gauge (LeVeen; Boston Scientific). Local application of 3 mL at 5–6 atm was performed during simultaneous balloon inflation with 3 atm for better wall contact and lasted 25–32 seconds. Digital subtraction angiography was performed after the end of the procedure.

Follow-up angiography before sacrifice was performed after laparotomy with the intravenous placement of a 20-gauge canule (Venflon; Becton Dickinson, Helsingborg, Sweden) in the proximal abdominal aorta with identical injection parameters as described earlier.

Digital subtraction angiograms were obtained with a dedicated scanner (Lumisys-20; Lumisys, Berkeley, Calif) and stored as tagged image file format (TIFF). Quantitative angiographic measurements were performed by using the Cardiovascular Angiographic Analysis System (CAAS; Pie Medical, Maastricht, the Netherlands) (18); the system was calibrated (M.C.) to the stent length of 15 mm. Mean luminal diameter within the stent region was calculated by the software following automatic edge detection. Preimplantation angiography with a calibrated grid was performed in five animals to determine the original vessel diameter.

Histomorphologic Evaluation, Morphometric Analysis, and Immunofluorescence

The vessel segments with stents were embedded en bloc in methylmethacrylate; then, three sections (proximal, middle, and distal part of the stent, each 500 μ m thick) were made with a diamond-wafering blade (Isomet; Buehler, Lake Bluff, Ill) and ground to about 50- μ m thickness. The surface of the polished ground sections was stained with Giemsa or van Giessen stain and evaluated at

light microscopy. Neointimal thickness was analyzed with quantitative histomorphometry. The images (AX70 microscope; Olympus, Tokyo, Japan, $\times 25$ magnification) were frame grabbed, and the picture was analyzed with an image analysis software (Analysis, Soft Imaging Software, Münster, Germany; or Osiris version 3.6, Digital Imaging Unit, University of Geneva, Switzerland). All images were coded after frame grabbing and analyzed by one investigator (M.C.) in a blinded fashion. The luminal area within the endothelial lining, the area within the internal elastic lamina, the internal elastic lamina border length, and the percentage of internal elastic lamina fracture length (fractured internal elastic lamina divided by total length) were measured. The neointimal area was then calculated (internal elastic lamina area minus luminal area).

Immunofluorescence was performed with monoclonal antibody to detect human I κ B α (sc-371 with epitope mapping of the carboxy terminus of human I κ B α ; Santa Cruz Laboratories) and GFP (*Aequorea victoria* origin; Santa Cruz Laboratories) on snap-frozen sections of treated vascular segments according to the manufacturer's recommendations. In the initial experiments, rAdCMV.GFP-treated vessels, as well as samples from liver, lung, and

kidney, were snap frozen and investigated for the presence of GFP expression.

Statistical Analyses

Data are given as mean \pm standard error of the mean. Statistical software (SPSS; SPSS, Chicago, Ill) was used for analyses. Bartlett test was used to confirm the null hypothesis of the homogeneity of variances. Comparisons of continuous variables among more than two groups were performed with a one-way analysis of variance (ANOVA) with Bonferroni correction and confirmed with the k-sample generalization of the two-sample Welch *t* test (19) and independent-sample *t* test to confirm significant differences among the individual groups (cited as *P* values, unless otherwise indicated). Data were considered significantly different if *P* < .05 was obtained.

RESULTS

Hypercholesterolemic Diet

After feeding with cholesterol and peanut oil, baseline levels of triglycerides increased from 48 mg/dL (0.54 mmol/L) \pm 8 to 142 mg/dL (1.6 mmol/L) \pm 37, and cholesterol levels increased from 221 mg/dL (5.7 mmol/L) \pm 27 to 2,628 mg/dL (68.0 mmol/L) \pm 248. After stent implantation,

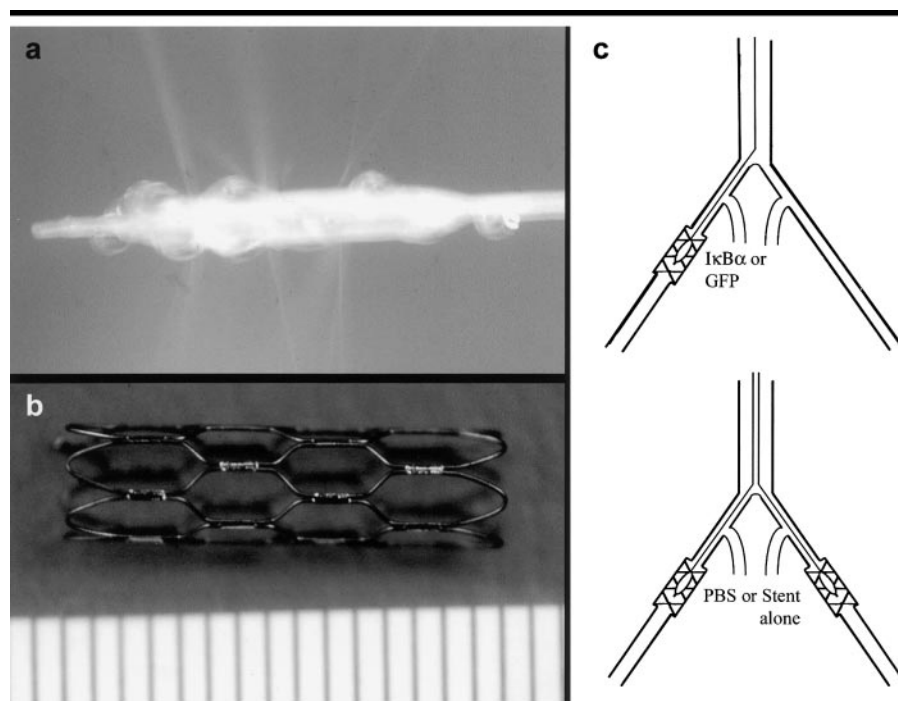


Figure 1. *a*, Self-expandable nitinol stent, 15 mm long and 3.5 mm in diameter. *b*, Multichannel balloon, 3 mm in diameter and 20 mm long. Local application of a viral solution or PBS was performed at 6 atm at a balloon pressure of 3 atm, which displayed a jet- and weepinglike application of the fluid. *c*, Schematics depict the experimental setup for virus-treated or control animals.

during the maintenance diet, triglyceride levels were 140 mg/dL (1.6 mmol/L) \pm 32 and cholesterol levels remained at 2,582 mg/dL (67.8 mmol/L) \pm 241.

Immunofluorescence and Transgene Expression

The initial experiments with the use of an adenovirus for the expression of GFP demonstrated a systemic effect, with GFP expression in liver, lung, and kidney (Fig 2) 1 week after adenovirus delivery. In the treated arteries, mainly smooth muscle cells of the media and cells of the adventitia were transduced, and GFP was detected at 1 week; no transgene was detected 4 weeks after the intervention. Immunofluorescence demonstrated trans-

gene expression ($\text{I}\kappa\text{B}\alpha$ and GFP) in the snap-frozen segments adjacent to the nitinol stent 1 week after treatment.

Effect of Gene Transfer on Neointimal Formation

No significant neointimal formation was observed in any experimental group 1 week after treatment (stent alone, 0.52 mm² \pm 0.09; stent plus PBS, 0.56 mm² \pm 0.07; and stent plus GFP, 0.42 mm² \pm 0.08). Only small accumulations of mainly mononuclear cells around the stent struts were observed without a statistically significant difference among the treatment groups ($P = .44$, ANOVA). Figure 3 demonstrates the typical presentation of control (stent alone) group versus that with $\text{I}\kappa\text{B}\alpha$

treatment 1 week after stent implantation. Internal elastic lamina fractures were found in only circumscribed areas (<2%), again with no significant differences among the groups.

Four weeks after implantation, there was marked neointimal formation for each treatment group ($n = 12$; stent alone, 2.80 mm² \pm 0.20; stent plus PBS, 3.26 mm² \pm 0.25) (Fig 4, Table 1), but neointimal formation was significantly reduced in $\text{I}\kappa\text{B}\alpha$ -treated arteries (2.28 mm² \pm 0.14, $n = 12$; $P = .05$ and $P = .002$, respectively). Consequently, the luminal area was significantly smaller in the stent alone group (2.95 mm² \pm 0.16) and in the stent plus PBS group (2.65 mm² \pm 0.19) than in the stent plus local delivery of $\text{I}\kappa\text{B}\alpha$ group (3.31 mm² \pm 0.10, $P = .08$ and $P = .005$, respectively) (Table 1).

Again at this time, there was no significant difference in the length of internal elastic lamina fractures among the groups (control, 10.8%; PBS, 15.4%; and $\text{I}\kappa\text{B}\alpha$, 18.5%; $P = .28$, ANOVA). The mean in-stent area was 6.01 mm² in the stent alone group, 6.20 mm² in the stent plus PBS group, and 5.87 mm² in the $\text{I}\kappa\text{B}\alpha$ group ($P = .20$, ANOVA). Figure 4 demonstrates the typical presentation 4 weeks after stent implantation and control (stent alone) versus stent plus $\text{I}\kappa\text{B}\alpha$ treatment. Comparison of rAdCMV.GFP versus rAdCMV. $\text{I}\kappa\text{B}\alpha$ confirmed these results with significant reduction of neointimal area (2.32 mm² \pm 0.19, $n = 9$ vs 1.51 mm² \pm 0.08, $n = 6$, respectively; $P = .005$) and increase in luminal area (4.40 mm² \pm 0.26, $n = 9$ vs 5.23 mm² \pm 0.13, $n = 6$, respectively; $P = .03$) after $\text{I}\kappa\text{B}\alpha$ treatment. Overall rAdCMV. $\text{I}\kappa\text{B}\alpha$ treatment reduced the neointimal area compared with stent alone (22%, from

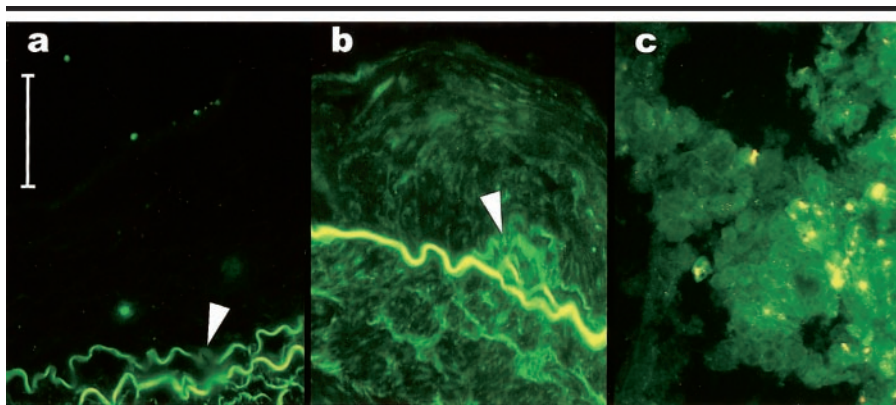


Figure 2. Representative photomicrographs of immunofluorescence-stained sections. *a*, PBS-treated control vessels do not express $\text{I}\kappa\text{B}\alpha$. $\text{I}\kappa\text{B}\alpha$ is expressed primarily by smooth muscle cells of transfected vessel segments. *b*, $\text{I}\kappa\text{B}\alpha$ transgene is expressed in a rabbit iliac artery 7 days after adenovirus-mediated gene transfer, as demonstrated with immunofluorescence detection of $\text{I}\kappa\text{B}\alpha$. Note the additional trauma in the dilated vessel areas treated with local drug delivery with partial disruption of the elastic membrane (arrowheads). The scale bar for *a* and *b* is 0.1 mm. *c*, On a photomicrograph, GFP transgene is expressed in rabbit liver 6 days after adenovirus-mediated gene transfer with immunofluorescence. (Original magnification, $\times 100$.)

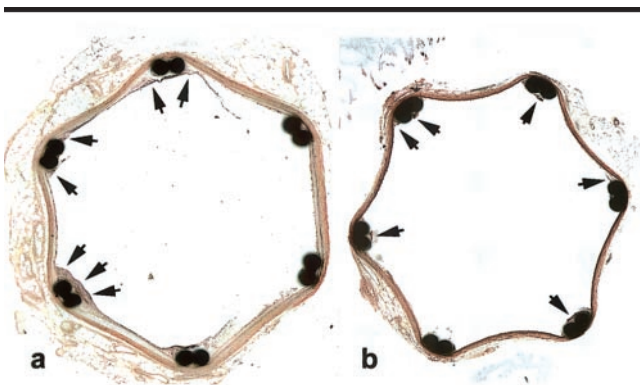


Figure 3. Representative photomicrographs of surface-stained ground sections. There is, as yet, no neointimal formation in the rabbit iliac artery with a stent on cross sections obtained 7 days after (*a*) stent placement alone or (*b*) gene transfer with $\text{I}\kappa\text{B}\alpha$. Only small cellular accumulations around the stent struts are seen in both samples (arrows). (van Giessen stain; original magnification, $\times 40$.)

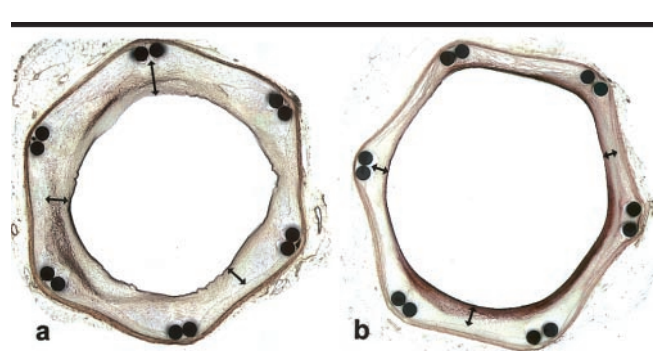


Figure 4. Photomicrographs of surface-stained ground sections obtained 4 weeks after stent implantation. *a*, Stent plus PBS treatment results in marked neointimal formation (arrows). *b*, Neointimal formation (arrows) is drastically reduced by the local delivery of rAdCMV. $\text{I}\kappa\text{B}\alpha$. The arrows delineate the extent of neointimal hyperplasia between the internal elastic lamina and the lumen in both samples. (van Giessen stain; original magnification, $\times 40$.)

2.80 mm² ± 0.20 to 2.28 mm² ± 0.14, *P* = .05), stent plus PBS (43%, from 3.26 mm² ± 0.25 to 2.28 mm² ± 0.14, *P* = .005), and stent plus GFP (53%, from 2.32 mm² ± 0.19 to 1.51 mm² ± 0.07, *P* < .005).

Quantitative Angiographic Analysis

In the initial experiments, the native external iliac artery diameter was 2.15 mm ± 0.1. The iliac artery and not the abdominal aorta was chosen for stent implantation to avoid potential stent-vessel diameter mismatch. Findings from quantitative angiography revealed an overstretch injury with a ratio of 1.3:1.5 after stent implantation and percutaneous transluminal angioplasty. Angiographically, no significant in-stent stenosis was found 1 week after treatment. The mean diameters of the vessels with stents were 3.47 mm ± 0.28 for stent alone (*n* = 4), 3.41 mm ± 0.20 for stent plus PBS (*n* = 3), 3.39 mm ± 0.49 for stent plus GFP (*n* = 3), and 3.31 mm ± 0.48 for stent plus IκBα (*n* = 3), with an overall *P* value of .96 with ANOVA. Four weeks after stent implantation, markedly reduced diameters were found for stent alone (2.77 mm ± 0.18, *n* = 3) and stent plus PBS (2.66 mm ± 0.26, *n* = 3) compared with stent plus IκBα (3.45 mm ± 0.71, *n* = 3). The overall *P* value of .12 with ANOVA was still not significant (Fig 5, Table 2).

DISCUSSION

The primary findings suggest that (a) local administration of the antiinflammatory protein IκBα by means of a recombinant replication-defective adenovirus successfully increases patent vessel luminal area after stent implantation in hypercholesterolemic rabbits, (b) this protective effect reduces the formation of neointima between 1 and 4 weeks after stent implantation, and (c) systemic transfection despite local application was demonstrated in this animal model.

To date, authors of experimental (6) and clinical (2,20) studies have suggested that inflammation and formation of intimal hyperplasia are even greater after stent implantation than after balloon angioplasty alone. Therefore, inflammation may be instrumental in the development of in-stent neointimal hyperplasia, and antiinflammatory agents may be useful in preventing in-stent restenosis. Prevention of inflammation and inhibition of smooth muscle cell proliferation may be key strategies for the prevention of restenosis in arteries with stents. Local deliv-

TABLE 1
Results of Histomorphometric Evaluation of 12 Sections
4 Weeks after Stent Implantation

Area (mm ²)	Mean	Standard Error of the Mean	Mean 95% CIs		Statistic
			Lower Bound	Upper Bound	
Lumen					
Stent	2.95	0.16	2.59	3.31	.02*
Stent plus PBS	2.65	0.19	2.24	3.07	1.00†
Stent plus IκBα	3.31	0.10	3.09	3.53	0.56†
Internal elastic lamina					0.075†
Stent	5.61	0.14	5.29	5.92	.92*
Stent plus PBS	5.68	0.15	5.36	6.00	NA
Stent plus IκBα	5.64	0.09	5.45	5.83	NA
External elastic lamina					NA
Stent	6.02	0.14	5.71	6.33	.20*
Stent plus PBS	6.18	0.13	5.90	6.46	NA
Stent plus IκBα	5.86	0.09	5.66	6.06	NA
Neointimal					<.01*
Stent	2.80	0.20	2.36	3.23	1.00†
Stent plus PBS	3.26	0.25	2.71	3.80	0.45†
Stent plus IκBα	2.28	0.14	1.96	2.60	0.045†

Note.—NA = not applicable.

* Number is the *P* value (ANOVA).

† Number is the *t* value for comparison with stent alone.

ery of NF-κB antisense oligonucleotides has proven effective in reducing neointimal formation after trauma to the rat carotid artery (21) but has never been tried to prevent neointimal formation after stent implantation. Stents have proven to be more effective compared with balloon angioplasty for the treatment of vascular stenosis because of a larger acute gain in vessel diameter (3,4). Until now, only the inhibition of smooth muscle cell proliferation was demonstrated to be an effective means for control of neointimal formation in animal stent models (22). Our approach was to induce an early inhibition of postinflammatory changes after vessel wall trauma (dilation plus stent insertion; and additional trauma, with fluid jets caused by local drug delivery) rather than direct inhibition of proliferation of smooth muscle cells (23).

Adenoviral vectors are useful for studies of injury-induced vascular hyperplasia because of their high transduction efficiency. These properties have resulted in optimistic predictions that adenoviral vectors may be used to deliver therapeutic genes to prevent restenosis after angioplasty (21,24,25). In contrast to local delivery of a drug, which is feasible only after or during the intervention and is then effective as long as its specific pharmacokinetics allows, transfection with an adenovirus results in expression of the transgene for as long as 14 days (24–27). However, a limitation of adenovirus-mediated gene therapy in humans is the prevalence of preexisting immunity to

adenovirus, which might lead to the destruction of adenovirus-transduced cells (26,27). Immune responses to adenoviral vectors are typically characterized by mononuclear cell infiltration, transgene elimination, and the inability to readminister the vector (26,27). In normal rabbit arteries, the adenovirus itself has an additional effect on vascular cell activation, which leads to signs of inflammation and an increase in neointimal hyperplasia (28). Other more inert vectors will be required for a more efficient transfection without the onset of an inflammatory response, although our approach of combining antiinflammatory gene therapy with an adenovirus could address this problem (21).

In our experimental setup, a demonstrable systemic effect was found 1 week after local delivery of an adenovirus construct for the expression of GFP. The amount of downstream decrease of virus will largely depend on the local drug delivery system, the amount of impregnated virus solution, and the duration of application and adaptation of the dilated balloon to the vessel wall. Still, the optimal approach for local drug delivery for arteriosclerotic human vessels with stents with diffuse wall thickening, circumscript, or diffuse calcifications has yet to be determined. These approaches will potentially differ from those demonstrated effective in the thin and yet only minimally changed rabbit vessels. In addition, different local application methods (24, 25,29–31) must be tested to eliminate

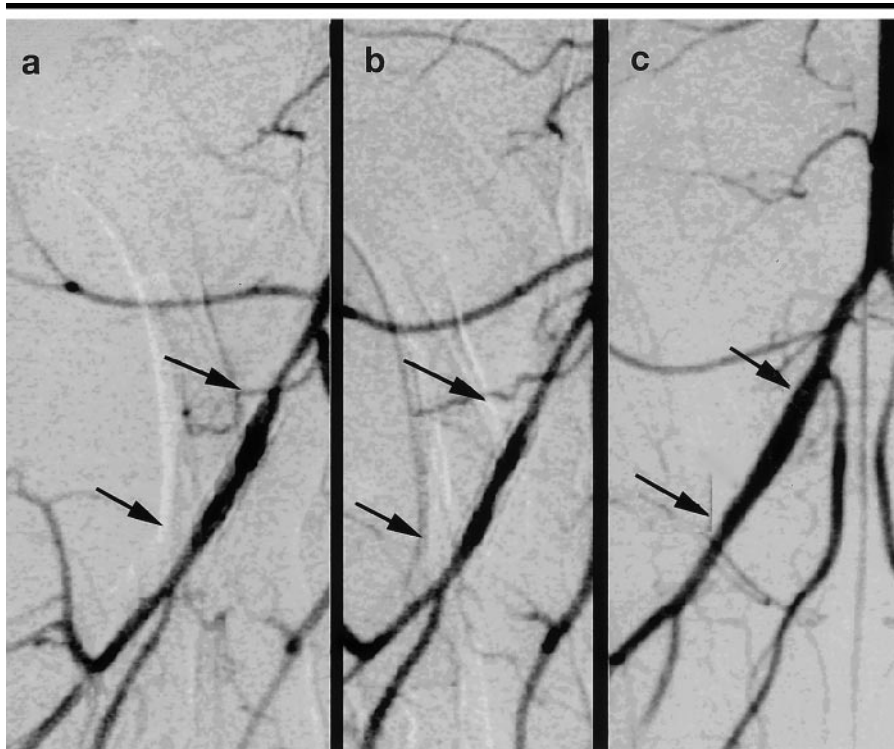


Figure 5. Representative digital subtraction angiograms at (a) 4 weeks after stent implantation alone, (b) stent plus PBS, and (c) stent plus I κ B α treatment. The arrows indicate the proximal and distal borders of the stent.

TABLE 2
Results of Quantitative Angiography after Stent Implantation

Patent Vessel Lumen Diameter (mm)	No. of Animals	Mean	Standard Error of the Mean
At 1 week*			
Stent	4	3.47	0.14
Stent plus PBS	3	3.41	0.11
Stent plus I κ B α	3	3.31	0.28
At 4 weeks†			
Stent	4	2.77	0.09
Stent plus PBS	4	2.66	0.13
Stent plus I κ B α	4	3.45	0.35

* P value of .96, ANOVA.
† P value of .12, ANOVA.

systemic transfection in a local therapy approach. Currently, new approaches with periadventitial delivery of gene therapy, which are feasible only with a surgical approach (28) and ultrasonographically enhanced gene delivery (30,31), seem to be the most promising to maximize local transfection and consequently minimize systemic delivery of gene therapy vectors.

One limitation of our study is the relatively small sample size, which resulted in reduced power of the statistical analysis, but our findings are confirmed by two independent sets of experiments. Another

limitation is that we implanted both virus-negative control groups in each control animal (with stent alone on the ipsilateral and stent plus additional local delivery of PBS on the contralateral side), although there were no considerations of potential reciprocal effects owing to the relative distance of the stents from the aortic bifurcation and the lack of virus treatment or additional medication.

Practical application: We plan to perform clinical pilot studies for the reduction of restenosis rates in areas such as the femoropopliteal region where stent placement has so far not been demon-

strated to be superior to angioplasty alone (32,33). A predominantly anti-inflammatory approach for the reduction of neointimal hyperplasia compares favorably with other methods as it reduces neointimal formation substantially (eg, radioactive stents [34] or local delivery of antiproliferative agents [35]), although the reported drawbacks of these approaches are delayed reendothelialization, with the potential complications of delayed thrombotic occlusions. In conclusion, our results suggest that inhibition of the posttraumatic inflammatory changes by the antiinflammatory proapoptotic protein I κ B α reduces neointimal formation after local therapy following stent implantation and might be an alternative approach to prevent in-stent restenosis.

Acknowledgments: The authors thank Prof Dr Kurt Hornik for statistical supervision; Mary McAllister, MA, for editorial assistance; and Birgit Lackner-Funovics, MD, for excellent assistance during interventional procedures and histologic work-up and for digitizing the histologic slides.

References

1. Clowes AW, Reidy MA, Clowes MM. Mechanisms of stenosis after arterial injury. *Lab Invest* 1983; 49:208–215.
2. Farb A, Sangiorgi G, Carter AJ, et al. Pathology of acute and chronic coronary stenting in humans. *Circulation* 1999; 99:44–52.
3. Serruys PW, de Jaegere P, Kiemeneij F, et al. A comparison of balloon-expandable-stent implantation with balloon angioplasty in patients with coronary artery disease. Benestent Study Group. *N Engl J Med* 1994; 331:489–495.
4. Fischmann DL, Savage MP, Leon MB, et al. Effect of intracoronary stenting on intimal dissection after balloon angioplasty: results of quantitative and qualitative coronary analysis. *J Am Coll Cardiol* 1991; 18:1445–1451.
5. Tanaka H, Sukhova GK, Swanson SJ, et al. Sustained activation of vascular cells and leukocytes in the rabbit aorta after balloon injury. *Circulation* 1993; 88:1788–1803.
6. Rogers C, Welt FG, Karnovsky MJ, Edelman ER. Monocyte recruitment and neointimal hyperplasia in rabbits: coupled inhibitory effects of heparin. *Arterioscler Thromb Vasc Biol* 1996; 16:1312–1318.
7. Rogers C, Edelman ER, Simon DI. A mAb to the beta2-leukocyte integrin Mac-1 (CD11b/CD18) reduces intimal thickening after angioplasty or stent implantation in rabbits. *Proc Natl Acad Sci U S A* 1998; 95:10134–10139.
8. Pietersma A, Kofflard M, de Wit LE, et al. Late lumen loss after coronary angioplasty is associated with the activation status of circulating phagocytes before treatment. *Circulation* 1995; 91:1320–1325.
9. Indolfi C, Avvedimento EV, Rapacciuolo A, et al. Inhibition of cellular ras prevents smooth muscle cell proliferation after

- vascular injury in vivo. *Nat Med* 1995; 1:541–545.
10. Varenne O, Pislaru S, Gillijns H, et al. Local adenovirus-mediated transfer of human endothelial nitric oxide synthase reduces luminal narrowing after coronary angioplasty in pigs. *Circulation* 1998; 98: 919–926.
 11. Janssens S, Flaherty D, Nong Z, et al. Human endothelial nitric oxide synthase gene transfer inhibits vascular smooth muscle cell proliferation and neointima formation after balloon injury in rats. *Circulation* 1998; 97:1274–1281.
 12. Sienbenlist U, Francesco G, Brown K. Structure regulation and function of NF-kappa B. *Ann Rev Cell Biol* 1994; 10:405–455.
 13. Wrighton CJ, Hofer-Warbinek R, Moll T, Eytner R, Bach FH, de Martin R. Inhibition of endothelial cell activation by adenovirus-mediated expression of I kappa B alpha, an inhibitor of the transcription factor NF-kappa B. *J Exp Med* 1996; 183: 1013–1022.
 14. Erl W, Hansson GK, de Martin R, Draude G, Weber KSC, Weber C. Nuclear factor-kappa B regulates induction of apoptosis and inhibitor of apoptosis protein 1 expression in vascular smooth muscle cells. *Circ Res* 1999; 84:668–677.
 15. Stehlik C, de Martin R, Kumabashiri I, Schmid J, Binder BR, Lipp J. Nuclear factor (NF)-kappa B-regulated X-chromosome-linked IAP gene expression protects endothelial cells from tumor necrosis factor alpha-induced apoptosis. *J Exp Med* 1998; 188:211–216.
 16. DeMartin R, Raidl M, Hofer E, Binder BR. Adenovirus mediated expression of green fluorescent protein. *Gene Ther* 1997; 4:493–495.
 17. Serruys PW, Foley DP, de Feyter PJ, eds. Quantitative coronary angiography in clinical practice. Dordrecht, the Netherlands: Kluwer Academic Publishers, 1994.
 18. Hong MK, Barry JJ, Leon MB. Multichannel balloon catheter. *Semin Intervent Cardiol* 1996; 1:34–35.
 19. Welch BL. On the comparison of several mean values: an alternative approach. *Biometrika* 1951; 38:330–336.
 20. Kearney M, Pieczek A, Haley L, et al. Histology of in-stent restenosis in patients with peripheral artery disease. *Circulation* 1997; 95:1998–2002.
 21. Autieri MV, Yue TL, Ferstein GZ, Ohlstein E. Antisense oligonucleotide to the p65 subunit of NF-kB inhibit vascular smooth muscle adherence and proliferation and prevent neointima formation in rat carotid arteries. *Biochem Biophys Res Commun* 1995; 213:827–836.
 22. Maillard L, Van Belle E, Tio FO, et al. Effect of percutaneous adenovirus-mediated Gax gene delivery to the arterial wall in double-injured atheromatous stented rabbit iliac arteries. *Gene Ther* 2000; 16: 1353–1361.
 23. Bellas RE, Lee JS, Sonenshein GE. Expression of constitutive NF-kB like activity is essential for proliferation of cultured bovine smooth muscle cells. *J Clin Invest* 1995; 96:2521–2527.
 24. Varenne O, Gerard RD, Sinnave P, Gillijns H, Collen D, Janssens S. Percutaneous adenoviral gene transfer into porcine coronary arteries: is catheter-based gene delivery adapted to coronary circulation? *Hum Gene Ther* 1999; 10:1105–1115.
 25. Palasis M, Luo Z, Barry JJ, Walsh K. Analysis of adenoviral transport mechanisms in the vessel wall and optimization of gene transfer using local delivery catheters. *Hum Gene Ther* 2000; 11:237–246.
 26. Yang Y, Nunes FA, Berencsi K, Furth EE, Gonczol E, Wilson JM. Cellular immunity to viral antigens limits E1-deleted adenoviruses for gene therapy. *Proc Natl Acad Sci U S A* 1994; 91:4407–4411.
 27. Schulick AH, Vassalli G, Dunn PF, et al. Established immunity precludes adenovirus-mediated gene transfer in rat carotid arteries: potential for immunosuppression and vector engineering to overcome barriers of immunity. *J Clin Invest* 1997; 97:209–219.
 28. Newman KD, Dunn PF, Owens JW, et al. Adenovirus mediated gene transfer into normal rabbit arteries results in prolonged vascular cell activation, inflammation and intimal hyperplasia. *J Clin Invest* 1995; 96:2955–2965.
 29. Schneider DB, Sassani AB, Vassalli G, Driscoll RM, Dichek DA. Adventitial delivery minimizes the proinflammatory effects of adenoviral vectors. *J Vasc Surg* 1999; 29:543–550.
 30. Lawrie A, Brisken AF, Francis SE, Cumberland DC, Crossman DC, Newman CM. Microbubble-enhanced ultrasound for vascular gene delivery. *Gene Ther* 2000; 7:2023–2027.
 31. Amabile PG, Waugh JM, Lewis TN, Elkins CJ, Janas W, Dake MD. High-efficiency endovascular gene delivery via therapeutic ultrasound. *J Am Coll Cardiol* 2001; 37:1975–1980.
 32. Cejna M, Thurnher S, Illiasch H, et al. PTA versus Palmaz stent placement in femoropopliteal artery obstructions: a multicenter prospective randomized study. *J Vasc Interv Radiol* 2001; 12:23–31.
 33. Grimm J, Muller-Hulsbeck S, Jahnke T, Hilbert C, Brossmann J, Heller M. Randomized study to compare PTA alone versus PTA with Palmaz stent placement for femoropopliteal lesions. *J Vasc Interv Radiol* 2001; 12:935–942.
 34. Drachman DE, Edelman ER, Seifert P, et al. Neointimal thickening after stent delivery of paclitaxel: change in composition and arrest of growth over six months. *J Am Coll Cardiol* 2000; 36:2325–2332.
 35. Tepe G, Dinkelborg LM, Brehme U, et al. Prophylaxis of restenosis with (186)re-labeled stents in a rabbit model. *Circulation* 2001; 104:480–485.